**Electronic supplementary materials** *Mendeleev Commun.*, 2017, **27**, 577–579

# Fullerene-mediated electrosynthesis of Ag–$C_{60}$ nanocomposite in a water-organic two-phase system

**Vitaliy V. Yanilkin, Natalya V. Nastapova, Gulnaz R. Nasretdinova, Rezeda R. Fazleeva, Aida I. Samigullina, Aidar T. Gubaidullin, Yakov V. Ivshin, Vladimir G. Evtugin and Yurii N. Osin**

## Experimental

The study was performed using cyclic voltammetry (CV), preparative electrolysis, transmission electron microscopy (TEM), powder X-ray diffraction (XRPD), dynamic light scattering (DLS) and ultraviolet-visible spectroscopy (UV/Vis).

***Reagents.*** Silver nitrate (Alfa Aesar), fullerene ($C_{60}$), $Bu_4NBF_4$, $NaBF_4$ (Fluka), 1,2-dichlorobenzene (DCB) (Alfa Aesar) were used without additional purification. Double distilled water was used.

***Cyclic voltammograms*** (CV curves) were recorded using a P-30J potentiostat (without IR compensation) in an argon atmosphere at potential scan rates 100 $mV \bullet s^{-1}$ in. A glassy carbon disc electrode (dia. 2.0 mm) sealed into a glass tube was used as the working electrode. Prior to each measurement, the electrode was mechanically polished. Platinum wire was used as the auxiliary electrode. Potentials were measured and reported *versus* an aqueous saturated calomel electrode (SCE) connected to the solution being studied through a bridge containing the supporting electrolyte and having a potential of -0.57 V relative to $E_0' Fc^{+/0}$ (internal standard). The temperature was 295 K.

***Preparative electrolysis*** was carried out in a three-electrode glass cell equipped with a diaphragm (porous glass), in potentiostatic mode (-0.38 V *vs*. SCE), in argon atmosphere at room temperature (T = 295 K) using a P-30J potentiostat. The solution was stirred with a magnetic stirrer during the electrolysis. A GC plate (S = 5.6 $cm^2$) was used as the working electrode and an SCE was used as the reference electrode. The latter was connected with the solution being studied through a bridge containing the reference electrolyte. A platinum wire immersed in the supporting electrolyte solution was used as the auxiliary electrode. After completion of the electrolysis, the resulting solution was studied by CV on a GC indicator electrode (dia. 2.0 mm).

To study the nanoparticles obtained in the electrolysis by TEM, XRPD, DLS and UV and visible spectroscopy they were precipitated by centrifugation (15 000 rpm, 1 h) from organic layer and washed with toluene, water and twice with ethanol. During the washing the deposit was dispersed in water by sonication and further reprecipitated by centrifugation (14 500 rpm, 30 min). Then the deposit was dispersed in ethanol by sonication.

In the case of TEM, 10 μl of the sample suspension was placed on a 3 mm copper mesh with formvar™/carbon support and dried at room temperature. After complete drying, the mesh in a special graphite holder was placed into a transmission electron microscope in order to perform the microanalysis.

***Electron microscopic analysis*.** The study by transmission electron microscopy was carried out in HR-TEM mode using a Hitachi HT7700 Exalens transmission electron microscope at accelerating voltage of 100 keV. Elementary analyses were carried out using Oxford Instruments X-Max$^n$ 80T attachment with a special holder.

The hydrodynamic diameter of the particles in solution was measured by **DLS**. The measurements were performed using Malvern Instrument Zetasizer Nano. The measured autocorrelation functions were analyzed with Malvern DTS software.

***UV/Vis spectra*** were recorded on a Perkin-Elmer Lambda 25 spectrometer.

***XRPD*** studies of the samples were performed on a Bruker D8 Advance automatic X-ray diffractometer equipped with a Vario attachment and a Vantec linear coordinate detector. Cu $K_{\alpha 1}$ ($\lambda$ 1.54063 Å) radiation monochromated by a curved Johansson monochromator was used. The operating mode of the X-ray tube was 40 kV, 40 mA. Room-temperature data were collected in the Bragg-Brentano geometry with a flat-plate sample.

A sample in liquid form was applied on a silicon plate that decreased background scattering. After drying of the layer, a few more layers were applied over it to increase the total amount of the sample. Patterns were recorded in the $2\Theta$ range between $3^o$ and $90^o$, in $0.008^o$ steps, with a step time of 0.1–5.0 s.

Processing of the data obtained was performed using EVA[1]. X-ray powder diffraction database PDF-2 (ICDD PDF-2, Release 2005-2009) was used to identify the crystalline phase.

Calculations of silver crystallite Ag(0) and silver chloride AgCl sizes carried out in several ways. The values calculated from reflections (LVol-FWHM) half-width and integrated reflections (LVol-IB) intensity are volume weighted values of crystallite sizes. The CrySizeL parameter is crystallite size in a direction perpendicular to the planes analyzed at Lorentz type broadening. Full-profile analysis of diffraction data by the Rietveld method was made using TOPAS software package[2]. Minimization in the process of the $R_{wp}$ and $R_{exp}$ convergence parameters verifying was used as a criterion of correct comparison of the calculated and

experimental data. The calculation of AgCl crystallite sizes was performed by the first three diffraction peaks [111], [200] and [220].

## References


1. *EVA v.11.0.0.3, User Manual*, SOCABIM, 2005.
2. *TOPAS V3, General profile and structure analysis software for powder diffraction data, Technical Reference*, Bruker AXS, Karlsruhe, Germany, 2005.


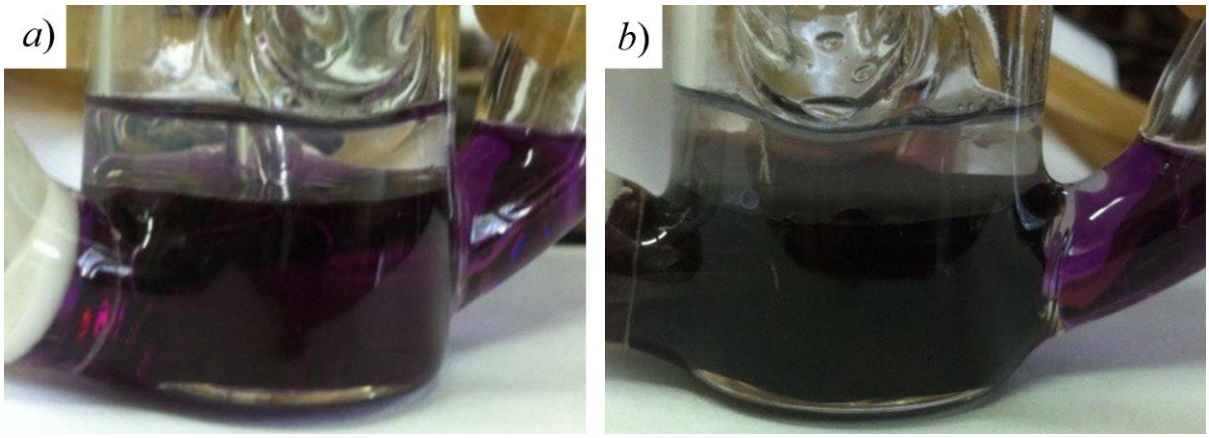


**Figure S1** Photos of the solution before (*a*) and after electrolysis (*b*).

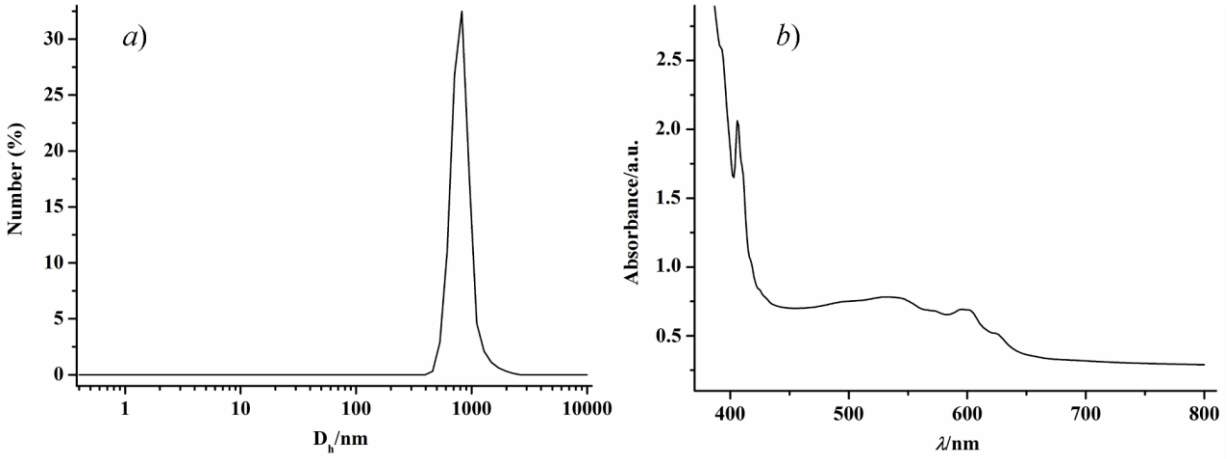


**Figure S2** Size distribution diagram (DLS data) (*a*) and absorption spectrum (*b*) of Ag@$C_{60}$ nanocomposite dispersed in ethanol.

**Table S1** Ag(0) crystallite sizes calculated from the parameters of interference peaks for the sample of **electrolysis 1.**

| **Miller indices of peak** | **111** | **200** | **220** | **311** | **222** |
|---|---|---|---|---|---|
| **degree 2θ, º** | 38.153(3) | 44.25(2) | 64.48(1) | 77.42(2) | 80.99(1) |
| **I (a.u.)** | 18.2(4) | 13.3(9) | 4.4(8) | 22(3) | 12(4) |
| **CrySizeL (nm)** | 26.4(8) | 9.5(8) | 45(11) | 13(2) | 33(4) |
| **LVol-IB (nm)** | 16.8(5) | 6.0(5) | 28(7) | 8(1) | 21(3) |
| **Lvol-FWHM (nm)** | 23.5(7) | 8.4(7) | 40(10) | 12(1) | 30(4) |
| **$R_{wp}$** | 3.59%. | | | | |
| **$R_{exp}$** | 3.33% | | | | |

**Table S2** Ag(0) crystallite sizes calculated from the parameters of interference peaks for the sample of **electrolysis 2.**

| **Miller indices of peak** | **111** | **200** | **220** | **311** | **222** |
|---|---|---|---|---|---|
| **degree 2θ, º** | 38.1382(9) | 44.304(4) | 64.486(4) | 77.423(4) | 81.55(1) |
| **I (a.u.)** | 49.5(3) | 26.2(5) | 22.9(8) | 34.9(9) | 8.4(9) |
| **CrySizeL (nm)** | 38.9(4) | 18.9(5) | 41(2) | 37(2) | 48(8) |
| **LVol-IB (nm)** | 24.8(2) | 12.1(3) | 26(1) | 24(1) | 31(5) |
| **Lvol-FWHM (nm)** | 34.6(4) | 16.9(4) | 36(2) | 33(1) | 43(7) |
| **$R_{wp}$** | 4.73%. | | | | |
| **$R_{exp}$** | 4.32% | | | | |

**Table S3** AgCl crystallite sizes calculated from the parameters of interference peaks for the sample of **electrolysis 1.**

| **Miller indices of peak** | **111** | **200** | **220** | **311** | **222** |
|---|---|---|---|---|---|
| **degree 2θ, º** | 27.819(3) | 32.232(1) | 46.220(3) | 54.782(8) | 57.455(9) |
| **I (a.u.)** | 3.9(2) | 6.8(2) | 7.2(3) | 2.5(3) | 2.9(4) |
| **CrySizeL (nm)** | 61(4) | 91(4) | 69(4) | 82(18) | 72(16) |
| **LVol-IB (nm)** | 38(3) | 58(2) | 44(3) | 52(11) | 46(10) |
| **Lvol-FWHM (nm)** | 54(3) | 81(3) | 62(4) | 73(16) | 64(14) |
| **$R_{wp}$** | 3.59%. | | | | |
| **$R_{exp}$** | 3.33% | | | | |

**Table S4** AgCl crystallite sizes calculated from the parameters of interference peaks for the sample of **electrolysis 2.**

| **Miller indices of peak** | **111** | **200** | **220** |
|---|---|---|---|
| **degree 2θ, °** | 27.817(3) | 32.220(1) | 46.202(3) |
| **I (a.u.)** | 2.6(1) | 7.8(2) | 6.2(2) |
| **CrySizeL (nm)** | 76(6) | 91(3) | 64(4) |
| **LVol-IB (nm)** | 48(4) | 58(2) | 41(2) |
| **Lvol-FWHM (nm)** | 67(6) | 81(3) | 57(3) |
| **$R_{wp}$** | 4.73%. | | |
| **$R_{exp}$** | 4.32% | | |

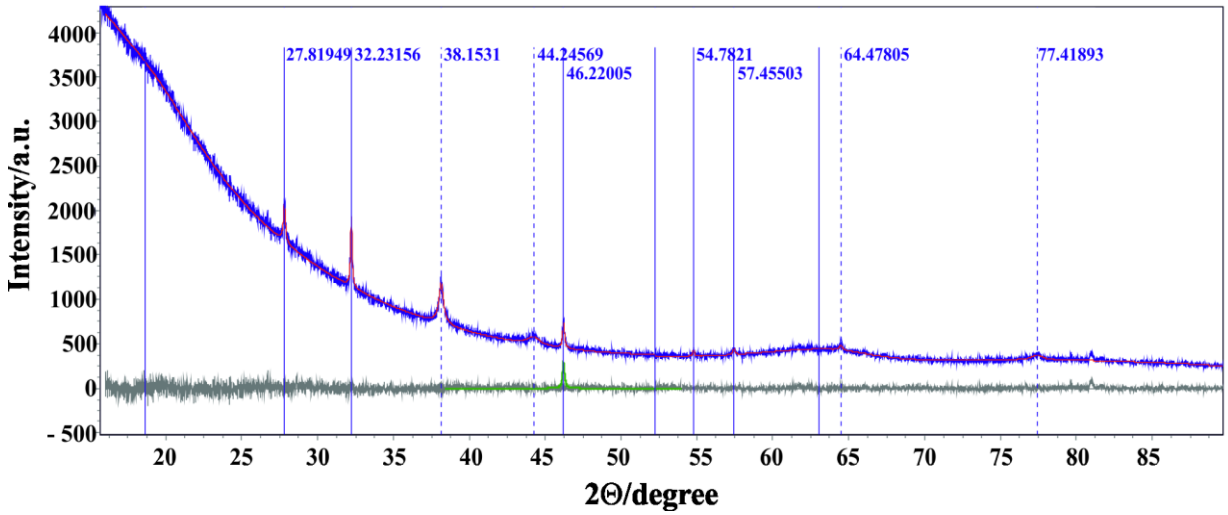


**Figure S3** The experimental powder diffraction pattern of the sample of **electrolysis 1.** The blue curve is the experimental diffraction pattern; the red curve is the theoretically calculated summary curve. The blue continuous vertical lines show the positions of the interference peaks corresponding to AgCl. The dashed vertical lines show the positions of the interference peaks of Ag(0). The gray curve is the residual difference curve.

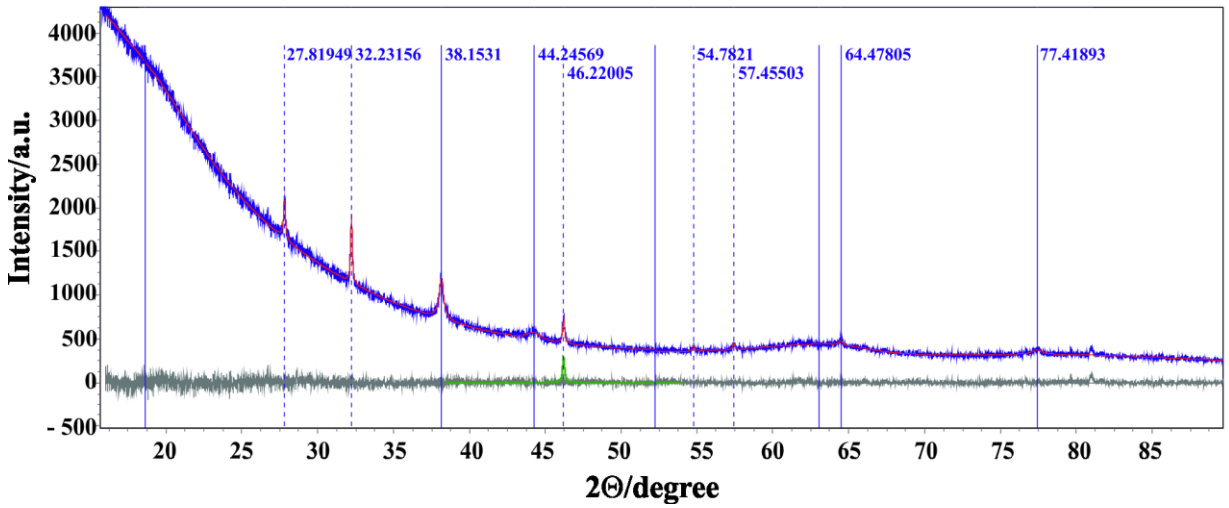


**Figure S4** The experimental powder diffraction pattern of the sample of **electrolysis 2.** The blue curve is the experimental diffraction pattern; the red curve is the theoretically calculated summary curve. The blue continuous vertical lines show the positions of the interference peaks corresponding to Ag(0). The dashed vertical lines show the positions of the interference peaks of AgCl. The gray curve is the residual difference curve.